Received: 2 April 2024 | Revised: 10 July 2024 | Accepted: 30 July 2024

DOI: 10.1111/gcb.17493

Global Change Biology WILEY

RESEARCH ARTICLE

Tall Bornean forests experience higher canopy disturbance rates than those in the eastern Amazon or Guiana shield

Toby D. Jackson[1,2] | Fabian J. Fischer[2] | Grégoire Vincent[3] | Eric B. Gorgens[4] | Michael Keller[5,6] | Jérôme Chave[7] | Tommaso Jucker[2] | David A. Coomes[1]

[1]Conservation Research Institute and Department of Plant Sciences, University of Cambridge, Cambridge, UK

[2]School of Biological Sciences, University of Bristol, Bristol, UK

[3]AMAP, Univ. Montpellier, CIRAD, CNRS, INRAE, IRD, Montpellier, France

[4]Departamento de Engenharia Florestal, Campus JK, Universidade Federal dos Vales do Jequitinhonha e Mucuri, Diamantina, Brazil

[5]USDA Forest Service, International Institute of Tropical Forestry, Rio Piedras, Puerto Rico, USA

[6]Jet Propulsion Laboratory, Pasadena, California, USA

[7]Centre de Recherche sur la Biodiversité et l'Environnement (CRBE), Université de Toulouse, IRD, Toulouse INP, Université Toulouse 3—Paul Sabatier (UT3), Toulouse, France

Correspondence
Toby D. Jackson and David A. Coomes, Conservation Research Institute and Department of Plant Sciences, University of Cambridge, Cambridge, UK.
Email: tobydjackson@gmail.com and dac18@cam.ac.uk

Funding information
Agence Nationale de la Recherche, Grant/Award Number: ANR-10-LABX-0041, ANR-10-LABX-25-01 and ANR-11-INBS-0001; Natural Environment Research Council, Grant/Award Number: NE/S010750/1, NE/S01537X/1 and NE/X000281/1; Leverhulme Trust, Grant/Award Number: RPG-2020-341

Abstract

The future of tropical forests hinges on the balance between disturbance rates, which are expected to increase with climate change, and tree growth. Whereas tree growth is a slow process, disturbance events occur sporadically and tend to be short-lived. This difference challenges forest monitoring to achieve sufficient resolution to capture tree growth, while covering the necessary scale to characterize disturbance rates. Airborne LiDAR time series can address this challenge by measuring landscape scale changes in canopy height at 1 m resolution. In this study, we present a robust framework for analysing disturbance and recovery processes in LiDAR time series data. We apply this framework to 8000 ha of old-growth tropical forests over a 4–5-year time frame, comparing growth and disturbance rates between Borneo, the eastern Amazon and the Guiana shield. Our findings reveal that disturbance was balanced by growth in eastern Amazonia and the Guiana shield, resulting in a relatively stable mean canopy height. In contrast, tall Bornean forests experienced a decrease in canopy height due to numerous small-scale (<0.1 ha) disturbance events outweighing the gains due to growth. Within sites, we found that disturbance rates were weakly related to topography, but significantly increased with maximum canopy height. This could be because taller trees were particularly vulnerable to disturbance agents such as drought, wind and lightning. Consequently, we anticipate that tall forests, which contain substantial carbon stocks, will be disproportionately affected by the increasing severity of extreme weather events driven by climate change.

KEYWORDS
Amazon, Borneo, canopy gaps, disturbance, LiDAR, recovery, tree mortality, tropical forest

1 | INTRODUCTION

The twentieth century carbon sink provided by tropical forests (Phillips et al., 2008) seems to have diminished in recent decades (Hubau et al., 2020; Mitchard, 2018). Part of this decrease was likely driven by the increased severity of extreme weather events (IPCC, 2021), which caused wide-spread disturbance in tropical forests (Berenguer et al., 2021; Leitold et al., 2018; Negrón-Juárez et al., 2010). The amount trees can grow each year is limited by their photosynthetic rate and resource availability (Cabon et al., 2022; Kannenberg et al., 2022), but forest disturbance and tree mortality have no such physiological limits. Therefore, an increase in the frequency or severity of disturbance events is likely to reduce the amount of carbon sequestered and stored by these forests (Muller-Landau et al., 2021). Unfortunately, forest disturbance and tree mortality processes are poorly represented in land surface models due to a lack of data (Bugmann et al., 2019) which limits our ability to predict how tropical forests will respond to climate change. We therefore urgently need to quantify disturbance and recovery processes in tropical forests.

Forest dynamics are often characterized as 'slow-in, rapid-out' (Körner, 2003). Trees grow slowly over decades, but rare disturbance events can devastate a patch of forest in minutes. This difference in scale makes it challenging to measure both disturbance and recovery processes in a consistent way. On one hand, traditional satellite remote sensing can map large (>0.1 ha) disturbance events (Reiche et al., 2021; Vancutsem et al., 2021), but they generally are not sensitive enough to measure the slow growth of canopy height (a few metres per year). On the other hand, field measurements can accurately quantify tree growth, but do not usually cover a large enough area and are not sampled frequently enough to reliably capture disturbance events. One way to overcome this limitation is to collate large networks of field plots, thus increasing the spatial coverage (Gloor et al., 2009). This method showed that tropical forests are net carbon sinks in central Africa (Bennett et al., 2021) and in South America (Bennett et al., 2023), except in El Niño years. Field measurements are extremely valuable and represent the work of thousands of people over many years (de Lima et al., 2022), but remote sensing methods are necessary to monitor forests at the landscape level.

Repeated airborne LiDAR scanning provides accurate measurements of canopy height and how it changes over time (Nunes et al., 2021; Silva et al., 2019). It is perfectly suited to detecting canopy gaps (Jucker, 2022), which are difficult to map in the field (Clark et al., 2022). Repeat LiDAR can therefore be used to efficiently scale-up the classic canopy gap dynamics analyses pioneered by Brokaw (1982) and Denslow (1987). This enables us to compare disturbance and recovery rates across sites (Gorgens et al., 2023; Hunter et al., 2015) and, in the long term, assess how forests are responding to climate change. At the landscape-scale, repeat LiDAR can be used to map the spatial patterns of disturbance and recovery, and how they vary with canopy structure and topography (Cushman et al., 2022). However, recent repeat LiDAR studies used different definitions of canopy gaps and disturbance events (Gorgens et al., 2022; Hunter et al., 2015; Leitold et al., 2022), which hinders our ability to generalize over time and space. Furthermore, repeat LiDAR studies on old-growth tropical forests have so far focused on the Americas and data from tropical Africa or Asia are lacking.

In this study, we provide a unified framework for analysing repeat LiDAR data and use it to compare disturbance and recovery rates in Borneo with those in the eastern Amazon and Guiana shield. We address the following three research questions:

Q1: Was disturbance balanced by recovery in old-growth tropical forests? We expect large variation at the plot scale (10 ha) due to the slow-in fast-out nature of forest dynamics, but this variation should balance out to roughly equilibrium at the site level (~1000 ha). We also expect the balance between disturbance and recovery to be impacted by the 2015–2016 El Niño event, which caused severe drought in Borneo and the eastern Amazon but not in the Guiana shield (Rifai et al., 2019).

Q2: Were disturbance and/or recovery rates in Borneo higher than those in the eastern Amazon and Guiana shield? The dipterocarp-dominated forests of Borneo are home to the tallest tropical trees (Ashton, 2014; Shenkin et al., 2019) and have high productivity (Banin et al., 2014; Piponiot et al., 2022). We therefore expect particularly high disturbance and recovery rates in these forests.

Q3: What drives the spatial variation in disturbance within each site? We expect higher disturbance rates due to wind, lightning and drought in (a) areas with taller trees (Gora & Esquivel-Muelbert, 2021) and (b) on exposed hilltops and ridges (Cushman et al., 2022; Muller-Landau et al., 2021).

2 | METHODS

2.1 | Study sites

We selected study sites in Borneo, eastern Amazonia and the Guiana shield (Figure 1). Combined, these sites cover over 8000 ha of old-growth humid tropical forest. All sites are located in strictly protected areas with no evidence of human disturbances, although we cannot rule out the possibility of illegal logging.

The two Bornean sites, Danum and Sepilok, are located within 100 km of each other in Sabah, Malaysia and have similar non-seasonal climates with approximately 2300 mm rainfall per year. They have rugged topography and are highly productive (Banin et al., 2014; Piponiot et al., 2022). They are dominated by the fast-growing trees from the dipterocarp family (Ashton, 2014) and the basal area-weighted wood density is substantially lower than in the Amazonian sites (Table 2) (Mitchard et al., 2014; Qie et al., 2017). Sepilok also contains a plateau with a distinct soil type and shorter, heath forest (Jucker, Bongalov, et al., 2018).

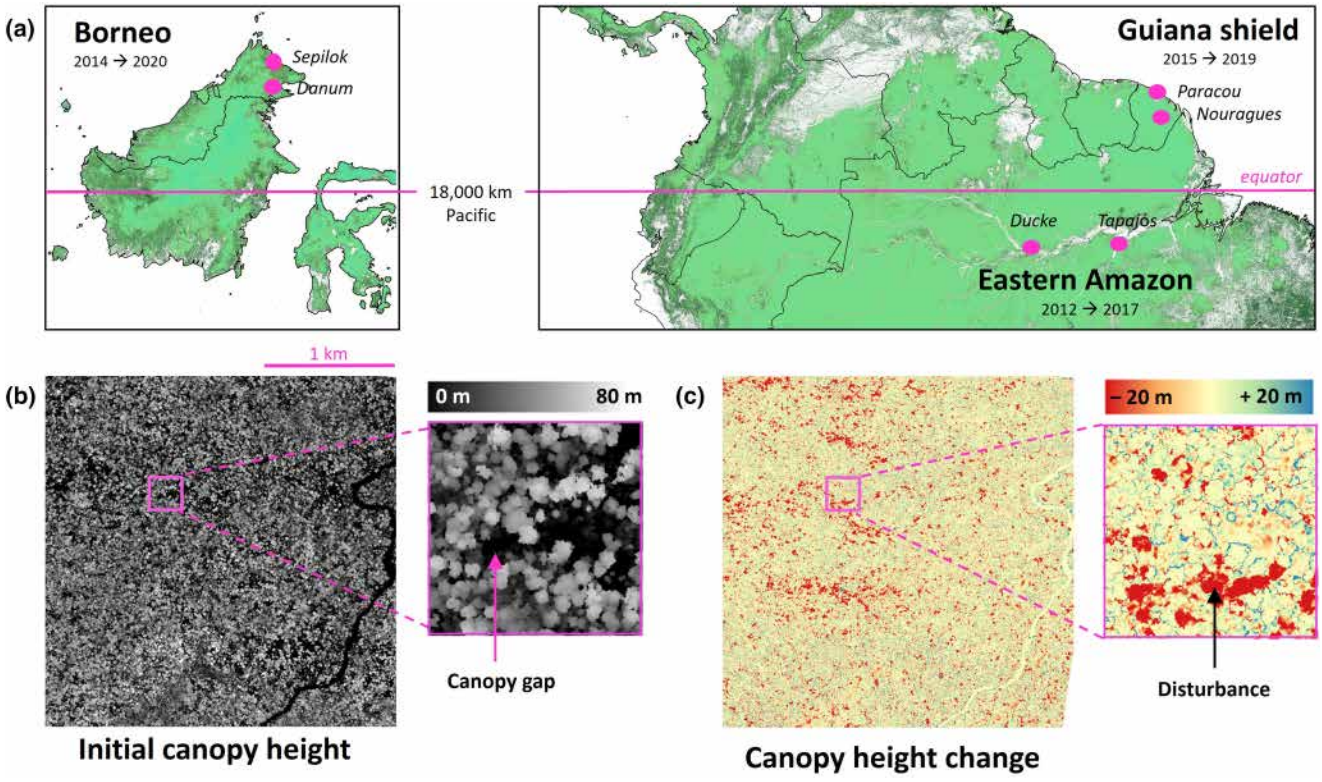

FIGURE 1 A map of the study sites and an example of the repeat LiDAR data used in this study. (a) Map of study sites overlaid onto forest cover map (green = forest and white = non-forest) derived from Global Ecosystems Dynamics Investigation data. (b) Example of canopy height rasters derived from LiDAR data from Danum, Malaysia. Smaller panels show a close-up of a 10-ha forest patch. (c) Canopy height change rasters for the same area as in (b). Map lines delineate study areas and do not necessarily depict accepted national boundaries.

The two sites in the eastern Brazilian Amazon vary considerably in their climatic conditions and forest structure. Adolpho Ducke (hereafter 'Ducke') is located in Amazonas State, near the city of Manaus with a mean annual temperature of 27°C and rainfall of 2194 mm. Tapajós is located in the eastern part of the Brazilian Amazon, in the state of Pará. It has an annual mean temperature of 25.1°C and rainfall of 2012 mm.

Compared to the rest of the Amazon, the forests of the Guiana shield have poorer soils (Quesada et al., 2010), higher wood density (Chave et al., 2009), slower growth rates (Chave et al., 2020) and are dominated by the Fabaceae family (ter Steege et al., 2006). We selected two sites in the Guiana shield, both located in French Guiana. Paracou is situated near the Atlantic coast and has a mean annual rainfall of approximately 3000 mm with a 3-month dry season from mid-August to mid-November (Wagner et al., 2012). It has very little topographic variation and a dense forest canopy. Nouragues, which is situated 100 km inland, has a similar climate but covers a much larger range of elevation (20–430 m asl).

These Amazonian sites cover a large area and range of climatic conditions, but they are not representative of the whole region. Specifically, we could not find any repeat LiDAR data available in the western Amazon, which has higher woody productivity (Malhi et al., 2004), potentially due to higher phosphorus availability (Quesada et al., 2010).

2.2 | LiDAR data collection and processing

In Danum and Sepilok, we collected airborne LiDAR data in October 2014 and again in February 2020 (Coomes & Jackson, 2022). In Paracou and Nouragues, we collected airborne LiDAR data in October 2015 and November 2019 (Jackson et al., 2023a, 2023b). In Ducke and Tapajós, we used available repeat LiDAR data from the Sustainable Landscapes Brazil programme, with flights in February 2012 and April 2017, and July 2012 and March 2017, respectively (dos-Santos et al., 2019). These dates were selected so that the interval between scans would be similar to that in Borneo. The interval between LiDAR scans varied from 4.16 to 5.36 years among sites (Supplementary material S1). The scanning was conducted at similar times of year whenever possible, to minimize the potential effects of leaf phenology on our results. We checked the aerial photographs collected alongside the LiDAR scans in Borneo for differences in phenology and found no evidence of this (Supplementary material S2). Detailed specification of all the LiDAR scans is given in Table S1.

The repeat LiDAR datasets used in this study represent the most robust way to measure changes in canopy height, particularly as these sites were selected due to their high data quality (Supplementary material S1). Instead of analysing the LiDAR point cloud, we built canopy height model (CHM) rasters at 1-m resolution to represent the canopy surface. In particular, we used a locally adaptive spike-free (lspikefree) method to build our CHM which was designed to be robust to variation in LiDAR scanning characteristics (Fischer et al., 2024). These CHMs are available online (Jackson et al., 2024). To focus the analysis-only over old-growth forest, we manually masked out all roads and rivers from the LiDAR data. We also masked out the experimental manipulations in Paracou using GPS coordinates of these plots and we masked out patches of bamboo as well as a non-forest rocky outcrop in Nouragues using a field verified map of these features.

2.3 | Framework for assessing canopy disturbance and recovery

Our aim was to study canopy dynamics using a framework that best distinguishes disturbance and recovery processes (Q1). In light of the sensitivity issues involved in estimating small changes in mean canopy height, we decided to distinguish the large disturbance events from the background growth in intact canopy. We also wanted to make full use of the repeat LiDAR data, while preserving a link to the rich history of research on canopy gap dynamics (Brokaw, 1982; Denslow, 1987). To this end, we developed the framework described in Table 1.

We initially subdivided the forest canopy into three categories: gaps, disturbances and intact canopy. We defined gaps as contiguous areas with an initial canopy height <10 m. We defined disturbances as contiguous areas where the canopy height decreased by 5 m or more between LiDAR scans. We set a minimum area threshold of 25 m^2 for both gaps and disturbances, but we give results using a 10 m^2 minimum area threshold in the Supplementary. We classified the remaining canopy area as 'intact canopy'. We then further subdivided the gaps and disturbances based on their canopy height in the second LiDAR survey. We subdivided gaps into those which recovered between LiDAR surveys (final canopy height >10 m) and those which persisted (final canopy height <10 m). We subdivided disturbances into those which created a new canopy gap (final canopy height <10 m) and those which occurred in the upper canopy (final canopy height >10 m). We tested the sensitivity of our results to these thresholds in Supplementary material S7.

Subdividing gaps and disturbances as described above has multiple advantages. Firstly, including canopy disturbance events captures an important component of canopy dynamics (Leitold et al., 2018; Marvin & Asner, 2016). Secondly, it enabled us to link our results to the literature by calculating traditional gap dynamics metrics such as the gap recurrence period (Denslow, 1987). The gap recurrence period was calculated using Equation (1) (Hunter et al., 2015). Finally, isolating disturbance events which create new gaps enabled us to test whether disturbance intensity varied with canopy height (Q3) without the confounding effect that disturbance events are naturally larger in taller forests. We would expect the total canopy volume disturbed to increase with canopy height simply because there is more canopy volume to lose in a taller forest. However, if the effect was simply due to canopy height, we would expect this increase to be confined to the disturbance events occurring in the canopy. Disturbance events which create a new gap (i.e. reach 10 m above the ground) should be rarer in a tall forest. Therefore, if total area of new gaps created increases (or the recurrence period decreases) with canopy height, we can be confident this result is robust.

TABLE 1 Framework for classifying canopy gaps and disturbance events.

	Initial canopy height	Height decrease	Final canopy height (m)
Gaps-recovered	<10 m	-	>10
Gaps-persistent			<10
Disturbances-canopy	-	>5 m	>10
Disturbances-new gap			<10
Intact canopy	All remaining canopy		

$$\text{Recurrence period} = \text{sampling interval} \times \frac{\text{area of initially intact canopy}}{\text{area of gaps formed between scans}} \tag{1}$$

For each class, we calculated the change in canopy volume by multiplying the area with the canopy height change. We then compare the changes in canopy volume in each class across the sites (Q2). Canopy volume change is closely related to biomass change (Jucker, Asner, et al., 2018), but we decided not to convert to units of biomass because this conversion would depend on assumptions about the stem size distribution, canopy packing and trees' wood densities, which are weakly correlated with the LiDAR measured canopy height. Canopy volume changes are more robust since they are directly measured by the LiDAR surveys. All data processing were carried out in R (R Core Team, 2021), primarily using the terra package (Hijmans et al., 2022) and the scripts are available online (Jackson, 2024).

2.4 | Spatial patterns of disturbance across the landscapes

All six repeat LiDAR surveys cover large and roughly rectangular areas. This allowed us to explore the spatial patterns of disturbance within each site. We split the rasters into 10-ha plots (316 m × 316 m) and built separate multiple linear regression for each site individually. We chose area disturbed as our response variable, rather than volume disturbed, to avoid confounding with canopy height.

We expected that the area disturbed would be larger in taller forests (Q3a). We used the maximum canopy height (99th percentile for robustness) instead of the mean because the latter is more influenced by the area of canopy gaps. We also hypothesized that the area disturbed would be larger in forests on steep slopes or on hilltops (Q3b). We therefore calculated the topographic position index (de Reu et al., 2013) and slope and for each site using a 30 m pixel size. Preliminary analysis showed that area disturbed was closely related to the initial gap fraction, so we also included gap fraction in the model. Finally, we included the pulse density increase between the two LiDAR scans in the model to control for this potential bias (Fischer et al., 2024). The resulting model is given in Equation (2).

$$\text{Area disturbed} \sim \Delta\text{pulse density} + \text{max height} + \text{elevation} + \text{gap fraction} \tag{2}$$

All predictor variables were centred and scaled before analysis. We graphically checked for co-linearity between predictor variables prior to modelling and found no strong evidence of this.

2.5 | LiDAR quality control and sensitivity analyses

Different LiDAR surveys will sample the canopy surface in different ways, leading to uncertainties and potential biases in canopy height estimates. In the following sensitivity analysis, we compare the robustness of the lspikefree CHM method with two commonly used methods, which we call the 'highest' and 'tin' CHM. The highest CHM method selects the highest point per square metre but is known to be sensitive to variation in pulse density (Roussel et al., 2017). The tin method uses a 2D Delaunay triangulation of the first returns to construct a Triangular Irregular Network (the 'TIN'), which is then mapped onto a 1 m grid. The tin CHM fits a surface to the mean height of first returns, which is not only more robust to sampling characteristics than the highest CHM, but it also samples small openings <1 m in extent. As a result, it does not represent the top of canopy height at 1 m scale, but rather the mean height at which light is first intercepted by the canopy (Fischer et al., 2024).

We focus our uncertainty analysis on the two sites in Borneo, Danum and Sepilok, since they have the largest difference in scanning characteristics (Table S1). The 2014 scan in Borneo was conducted from an aeroplane flying at approximately 1800 m over Sepilok and 2300 m over Danum, while the 2020 scan used a helicopter flying at 250 m over both sites. This difference in altitude resulted in LiDAR datasets with different characteristics. Below, we discuss a number of potential biases, alongside the sensitivity analyses, we conducted to address them.

A *Pulse density*. Pulse density is the primary measure of LiDAR data quality (Fischer et al., 2024). We filtered the data to only include areas where both 2014 and 2020 scans had more than two pulses per square metre, as recommended in Fischer et al. (2024), to isolate other potential biases from the effect of pulse density. In Danum, the lspikefree estimate of canopy height difference was 0.24 m greater after filtering for pulse density (Supplementary material S5). The highest raster method was substantially more sensitive to this filter (+0.98 m), but the 'tin' raster method was more robust (+0.03 m). The Sepilok estimates were largely unchanged by this filter because most of Sepilok has more than two pulses per square metre.

B *Scan angle*. The lower altitude 2020 scan used a wider scan angle than the 2014 scan, which may miss the top of the canopy in some areas. We therefore filtered the data to areas where both scans had a scanning angle under 10°. The canopy height change estimates calculated using the lspikefree raster method were robust to this filter (<0.1 m difference in both sites, Supplementary material S5).

C *Footprint size*. The high altitude 2014 scans had a larger LiDAR footprint size than the 2020 scan. A larger footprint size could lead to lower canopy height estimates because the first maximum of the returned energy is lower (Roussel et al., 2017), or higher canopy height estimates, because it is more likely to sample the tallest parts of the canopy and has a greater horizontal uncertainty about the location of the return, which results in a 'smoother' canopy height model. The effect of footprint size was isolated in Sepilok in 2014 by scanning the same area twice in 1 day at altitudes of from 800 m and 1800 m, keeping pulse density constant (Supplementary material S6). This showed that the lspikefree and highest canopy height estimates were 0.36–0.38 m higher in the high-altitude scan compared to the low altitude scan. The tin method had a larger bias (+1.03 m). This positive bias likely impacts our comparison of the high altitude 2014 scan with the low altitude 2020 scan (the difference in footprint size is similar), but the 2020 scan had a much higher pulse density which may counterbalance this bias to some extent by sampling a larger area of the canopy.

D *Horizontal alignment*. In all cases, the scans were geo-referenced by the provider using ground control points accurately located with a differential GPS. We confirmed the alignment of the scans by comparing the positions of fixed features such as buildings (Supplementary material S3).

E *Ground detection*. We calculated the canopy height change as the difference between canopy height models, where each scan was normalized by its own terrain model. However, there is some uncertainty in the terrain models which interacts with LiDAR scanning characteristics. We therefore calculated the difference between the 2014 and 2020 terrain models as a component of the uncertainty in canopy height change. The results showed a mean increase in ground elevation of 0.3 m in Danum and 0.5 m in Sepilok (Supplementary material S4).

F *Combined effects*. In addition to the differences in scan angle, footprint size and pulse density, the 2014 and 2020 scans were conducted using different LiDAR scanners (Leica ALS50-II and Riegl LMS-Q560, respectively). These LiDAR scanners have different characteristics including the wavelength and the method used to discretize the returned waveform into a discrete point cloud. Fortunately, an additional scan was conducted in a small area of Danum in 2013 using the same scanner and similar scanning characteristics as the 2020 scan. In this area, the lspikefree canopy height estimate from the high altitude 2014 scan was 0.69 m higher than the low altitude 2013 estimate (Supplementary material S6). This is not a perfect control, since the actual canopy height may have changed in between these scans, but it this gives an estimate of the scale of bias to expect when comparing the LiDAR scans in Danum and Sepilok.

In summary, our sensitivity analysis shows that the 'lspikefree' raster method was the most robust to the variation in scanning characteristics. However, we still expect a negative bias of up to 0.7 m in the 2020 canopy height estimates due to the different scanning characteristics (point F). These results are in line with previous studies, which found small biases, both positive and negative, in canopy height with LiDAR beam footprint size (Goodwin et al., 2006; Morsdorf et al., 2008; Næsset, 2009; Roussel et al., 2017).

3 | RESULTS

3.1 | Mean canopy height changes

Our repeat LiDAR estimate of mean top-of-canopy height remained stable in eastern Amazonia and the Guiana shield but decreased in Borneo. We estimate a 2 m decrease in Danum (0.38 m per year) and a 0.78 m decrease in Sepilok (0.15 m per year). However, the magnitude of these height changes may be overestimated by up to 0.7 m, due to differences in scanning characteristics between the 2014 high altitude scan and the 2020 low altitude scan (see Section 2.5; Supplementary material S2–S6).

Focusing on changes in mean top-of-canopy height overlooks the dynamic processes of disturbance and recovery. In all sites, most of the forest canopy grew taller (medians were consistently positive), but all sites also showed evidence of large height losses through disturbance (long tails to the left, Figure 2b). This suggests a widespread growth in canopy height, approximately balanced by disturbance events (Q1). In the following sections, we disentangle the effects of disturbance and recovery using the framework described in Section 2.3.

3.2 | Site-level canopy disturbance and recovery rates

Across all sites, disturbance events caused a large loss of canopy volume (Figure 3a), despite covering a small proportion of the canopy area (7%–25%, Figure 3b). In fact, the majority of canopy volume loss was contained in disturbance events smaller than 300 m^2, but bigger than our minimum threshold of 25 m^2 (Figure S7.2). Canopy volume recovery rates were relatively similar across all sites (Table 2) and were sufficient to balance out the disturbance in the eastern Amazon and Guiana Shield, but not in Borneo (Q1). In all sites, canopy volume growth was dominated by intact canopy, because this class makes up the vast majority of the canopy area (Figure 3b). Growth rates in the canopy gaps were significantly faster than the growth in the intact canopy (Table 2) because this represents the recovery of recently disturbed forests. However, canopy gaps cover a small area, so the canopy volume change due to this growth was small.

We found that taller sites experienced more disturbance (Q2), both in terms of canopy volume (Figure 3a) and canopy area (Figure 3b). Tall sites also had faster gap recurrence rates, caused by the higher disturbance rates (Table 2). This demonstrates that the larger volume disturbed in taller forests was not simply because these forests have larger initial volume. In these tall forests, more canopy volume must be lost to reach the 10 m height threshold for canopy gaps. A constant disturbance rate (i.e. proportion of canopy affected by a height drop >5 m) would therefore result in fewer new gaps in taller forests, and a longer gap recurrence time. The fact that we found a shorter gap recurrence time demonstrates that the trend of increasing disturbance with canopy height was robust.

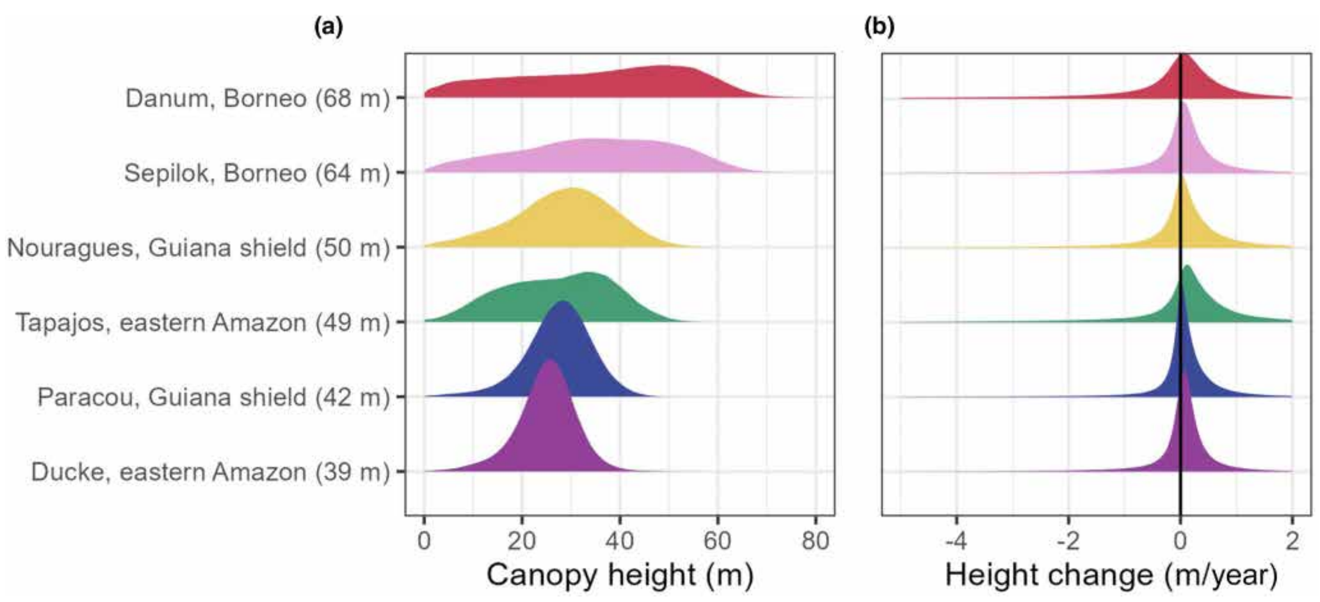

FIGURE 2 (a) Canopy height distribution in the first LiDAR scan. (b) Canopy height change over the 4–5-year periods. The sites are ordered by the 99th percentile of canopy height (given in brackets).

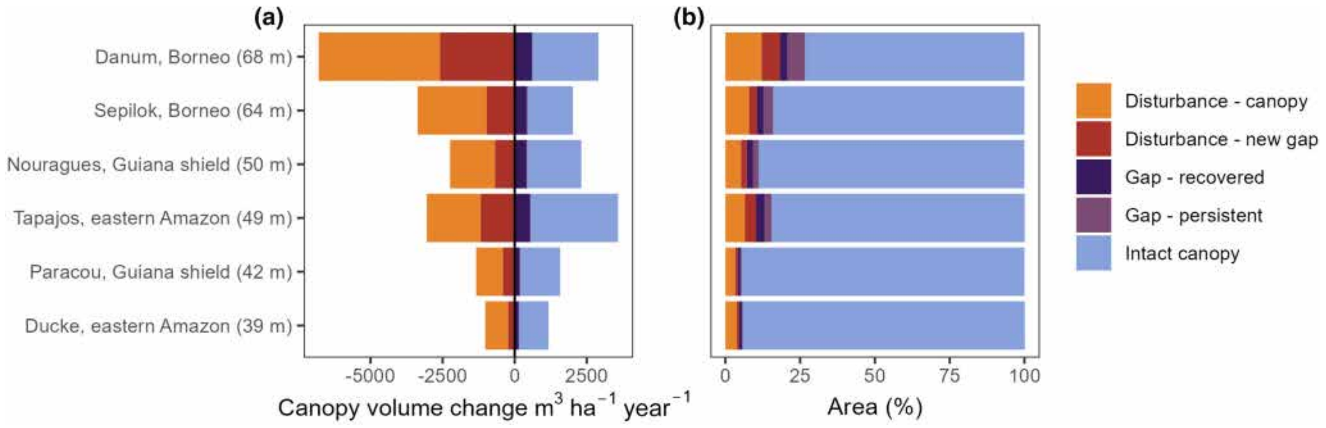

FIGURE 3 Comparing disturbance and recovery rates across sites. (a) Canopy volume change for each canopy class. (b) Percentage of the site area contained in each canopy class. The sites are ordered by the 99th percentile of canopy height (given in brackets).

TABLE 2 Overview of the study sites, their canopy gap dynamics and recovery rates.

Site	Area (ha)	Canopy height (m, 99th percentile)	Basal area weighted wood density	Gap recurrence period (years) (from Equation 1)	Mean disturbance size (m^2)	Growth rate (m/year)	
						Gaps	Intact canopy
Danum	1509	68	0.54	80	155	0.86	0.35
Sepilok	1779	64	0.59	184	107	0.99	0.26
Nouragues	2172	50	0.67	221	105	1.54	0.23
Tapajós	879	49	0.68	117	117	1.18	0.47
Paracou	657	42	0.70	573	103	1.47	0.15
Ducke	1088	39	0.73	726	91	1.22	0.28

3.3 | Was disturbance balanced by recovery at the 10-ha scale?

We subdivided the LiDAR scans into plots to test whether disturbance and recovery were balanced at the 10-ha scale (Q1). The sites in the eastern Amazon and Guiana shield generally clustered around the equilibrium line, meaning that disturbance was balanced by recovery at the 10-ha scale (Figure 4a). However, the Bornean sites were clustered underneath (Figure 2a) or to the left of (Figure 2b) the equilibrium line, meaning that disturbance outpaced recovery rates in the majority of 10-ha plots. We also observed that the largest decreases in canopy height occurred in the tallest 10-ha plots (Q3b, Figure 4b).

3.4 | Modelling the spatial variation in disturbance within sites

We ran multiple linear regression models (Figure 5) at the 10-ha scale to understand how the area disturbed (combining both canopy disturbance and new gaps) varied across each site. In three of the six sites, the model showed moderate predictive power (Tapajós $R^2=0.35$, Nouragues $R^2=0.53$ and Sepilok $R^2=0.55$). The model had low predictive power in Paracou and Ducke ($R^2=0.19$ and $R^2=0.23$, respectively) and very low in Danum ($R^2=0.06$). Excluding Danum, we found that the effect of LiDAR pulse density was not significant, showing that the trends we observed were robust to the primary source of sampling bias.

In Sepilok, Nouragues and Ducke, we found a significant increase in area disturbed with maximum canopy height (Figures 5 and 6a). The same trend (although non-significant) was also detected in Paracou and Tapajós. This aligns with our expectation that taller forests will experience more disturbance (Q3a), which could be due to a greater vulnerability to drought, wind and lightning. However, this trend was not observed within Danum, presumably because the range of maximum canopy heights was relatively low (Figure 6a).

Contrary to our expectation (Q3b), we found that disturbance rates were not strongly or consistently related to topography (Figures 5 and 6b). We tested slope, elevation and topographic position index and found weak and contradictory trends between sites. We therefore used elevation in the final model, which is simpler because the other metrics vary with the spatial scale at which they are calculated. Note that we found a significant effect of elevation in Tapajós, but this site is almost completely flat (Figure 6b) so we cannot interpret this as ecologically meaningful. We did find a strong effect of elevation on disturbance in Sepilok, but we believe that this is likely due to differences in forest type rather than increased exposure to wind, lightning or drought (discussed in Section 4.3).

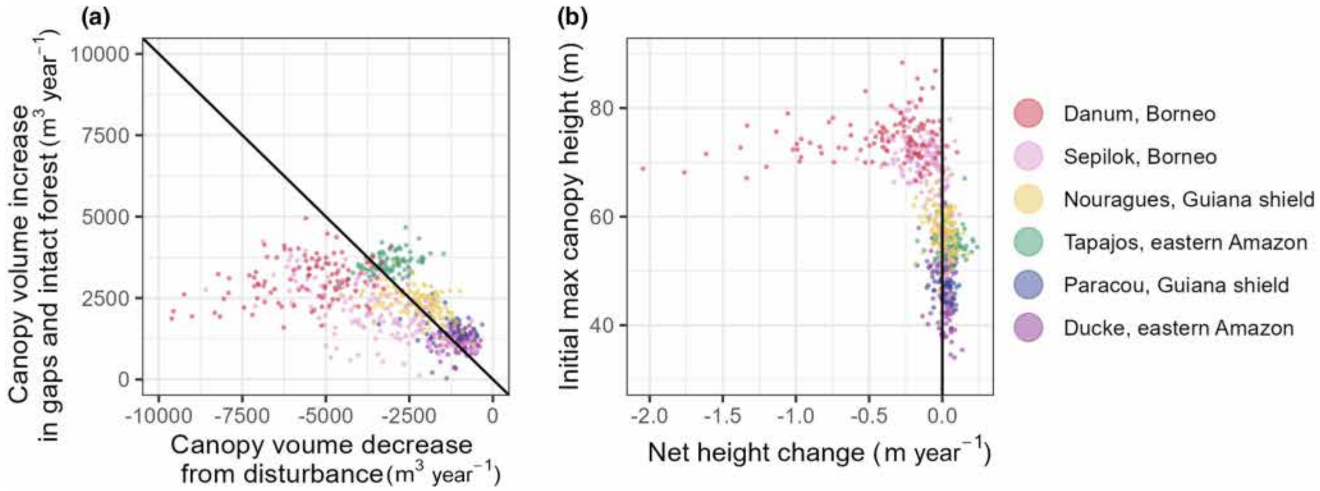

FIGURE 4 Taller forests experienced the largest decrease in canopy height, both within and across sites. (a) Changes in canopy volume changes due to disturbance and recovery at the 10-ha scale within each site. (b) Net height changes against initial maximum canopy height at the 10-ha scale. The black lines in both figures represent the equilibrium line (i.e. no net change in canopy volume or height). Each point represents a 10-ha plot.

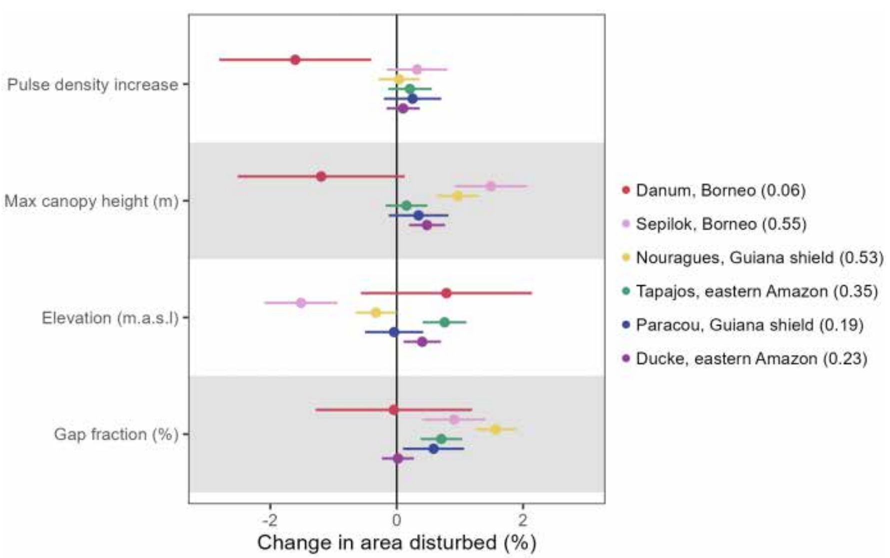

FIGURE 5 Normalized effect sizes from multiple linear regression models of area disturbed for each site at the 10-ha scale. The points show the mean effects, and the whiskers show the 95% confidence intervals. The model coefficient of determination (R^2) for each model is given in parentheses in the legend.

Surprisingly, we found that the area disturbed was positively correlated with initial gap fraction in four of the six sites (Figure 5), as well as across sites (Figure 6c). This is despite the fact that these classes (canopy gaps and disturbances) are mutually exclusive in our analysis framework. This means that, if the location of disturbance events was random, we would expect negative correlations between them. The positive relationships therefore show that disturbances occur more often in areas of forest which have experienced previous disturbance leading to canopy gaps.

4 | DISCUSSION

We provide the first landscape-scale comparison of disturbance and recovery rates between forests in Borneo, the eastern Amazon and the Guiana shield. We used repeat LiDAR to measure fine-scaled changes in canopy height over a 4–5-year period covering 8000 ha of old-growth humid tropical forest. Our results show that recovery rates were relatively similar across all sites, but that the tall forests of Borneo suffered particularly high disturbance rates.

4.1 | Slow-in, rapid-out forest dynamics

Across all sites, most of the forest canopy area remained intact and grew taller over time. However, this large-scale canopy growth was effectively counterbalanced by a large number of small disturbance events (Q1). This pattern is characteristic of the 'slow-in, rapid-out' forest dynamics described by Körner (2003).

Canopy growth rates were relatively similar across sites, presumably because trees have similar photosynthetic rate (Muller-Landau et al., 2021). This is despite the fact that field

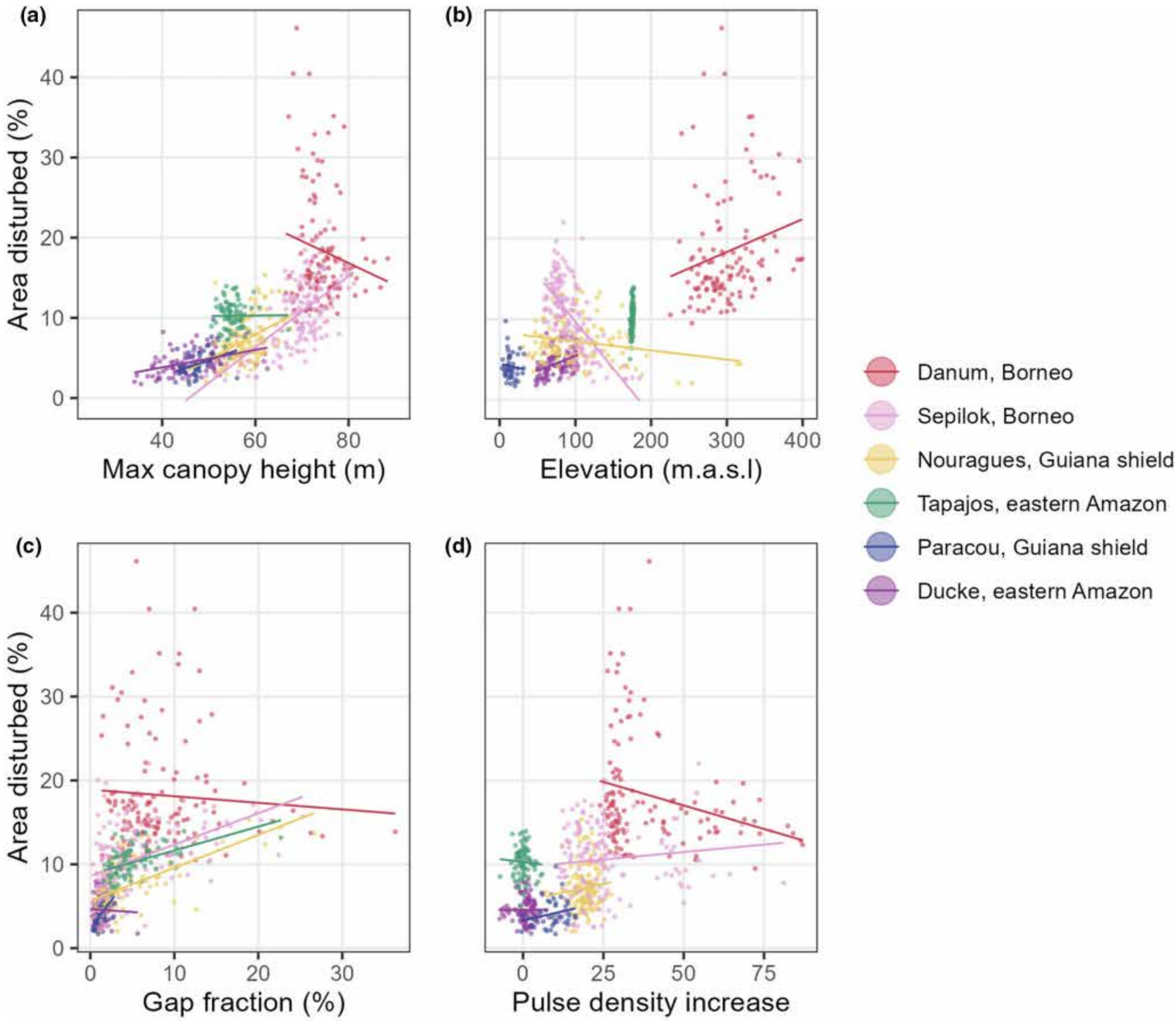

FIGURE 6 Area disturbed against (a) maximum canopy height, (b) elevation, (c) initial gap fraction and (d) increase in LiDAR pulse density between scans. Each point represents a 10-ha plot, and the lines are bivariate linear regressions displayed to help visualize the data.

data has shown Borneo to have higher productivity than the eastern Amazon and Guiana shield (Banin et al., 2014; Piponiot et al., 2022). This discrepancy could be simply due to the fact that field data measures changes in tree trunk diameter, while LiDAR measures changes in canopy height. The two measures are not necessarily correlated for tall trees, because they may allocate resources to reproduction, crown expansion or root growth, rather than height growth.

The mean size of a disturbance event ranged from 91 m^2 in Ducke to 155 m^2 in Danum (Table 2). In total, around 10%–25% of the canopy area was disturbed in each site, but the canopy volume loss in these disturbance events was similar to the growth in the remaining 75%–90% of the forest canopy in the sites in the eastern Amazon and Guiana shield but larger in Borneo. Because canopy volume change is closely related to carbon dynamics (Jucker, Asner, et al., 2018), we confirm previous findings that a large proportion of the forest carbon dynamics occur in small disturbance events (Espírito-Santo et al., 2014). The majority of these small disturbance events would have been missed by traditional satellite disturbance trackers, because they have a minimum mapping unit of approximately 1000 m^2 (0.1 ha) (Reiche et al., 2021; Vancutsem et al., 2021). This emphasizes the need for additional data, such as LiDAR or high-resolution (<5 m) satellite imagery to track canopy disturbance over time (Dalagnol et al., 2023).

4.2 | Tall Bornean forests suffered the highest levels of disturbance

Taller forests experienced higher disturbance rates, both across sites and within each site (Q3a). This may be due to the greater vulnerability of tall trees to wind (Jackson et al., 2020), drought and lightning (Gora & Esquivel-Muelbert, 2021). Danum, which is home to the tallest trees in the tropics (Shenkin et al., 2019), had the highest disturbance rates in this study and experienced an overall decrease in canopy height (although mean canopy height changes were sensitive to LiDAR processing methodology). Danum also had the shortest gap recurrence time of 80 years, compared to 117–726 years across the other five sites. Together, these results suggest that taller forests suffered from increased disturbance and did not adequately recover during the study period. Because the rates of disturbance vary dramatically while recovery rates are limited by tree growth rates (Muller-Landau et al., 2021), we expect this reduction in canopy height to be exacerbated by the effects of climate change.

The 2015–2016 El Niño event caused a severe drought in Borneo and eastern Amazonia, but not in the Guiana shield (Rifai et al., 2019). Our repeat LiDAR results show that canopy height remained roughly stable over time in the Guiana shield, which may be expected given the low turnover rates in these forests (Chave et al., 2020). However, we also found no substantial change in canopy height in the eastern Amazon, despite the fact that the second LiDAR measurement was conducted in 2017, only 1 year after the peak of the El Niño event. This suggests that the forests in Ducke and Tapajós recovered their canopy structure quickly after this drought. Field measurements show that tree trunk diameter growth rates slowed in the regions most affected by the drought (Rifai et al., 2018), but this seems to have had little knock-on effect on canopy structure in over the period of our study. This overall stability in canopy height suggests that these forests were neither a large source nor a large sink of carbon over this period, which is in agreement with results from field data (Hubau et al., 2020). We note that the comparison of disturbance and recovery between sites is complicated by the opportunistic nature of our sampling resulting in different dates for the LiDAR surveys.

4.3 | Disturbance was weakly related to topography

We expected strong topographic trends in disturbance rates (Q3a) driven by increased exposure to wind, drought and lightning on the ridges and hilltops (Cushman et al., 2022; Muller-Landau et al., 2021). However, we found that disturbance rates were only weakly related to topography (we tested slope, topographic position index and elevation). This could be because the processes we expected to be driving disturbance (wind, drought and lightning) were less topographically structured than we had assumed, or that the disturbance was driven by other processes which we had not considered.

We did find a strong effect of elevation on disturbance rates in Sepilok. However, the forest in Sepilok changes from dipterocarp-dominated forest on the low elevation alluvial soil (similar to Danum) to heath forest on sandy soil on the nearby plateau (Jucker, Bongalov, et al., 2018). We therefore believe this change in disturbance rate is likely due to soil type and forest structure, rather than being a true effect of topography driven by the mechanisms we were intending to explore (e.g. increased wind and lightning exposure). We note that some of the sites had relatively flat terrain, so no topographic trend was expected in these sites.

Intriguingly, we found that disturbance was higher in areas which had larger initial gap fractions (i.e. areas which had previously suffered more disturbance). This suggests a compounding effect often referred to as 'gap contagiousness', whereby the initial disturbance changes the local microclimate (e.g. increasing wind exposure of the remaining trees) and thus increases the risk of future disturbance. There is strong evidence of gap contagiousness in some temperate forests (Krüger et al., 2024), but no strong effects have been found in tropical forests (Hunter et al., 2015; Jansen et al., 2008). We were therefore surprised by this result, particularly as the two classes (initial gaps and disturbance) are mutually exclusive in our framework, so we would have expected a negative relationship between them by default. Another possibility is that some underlying driver, perhaps related to water availability or soil fertility, increases the local productivity leading to higher growth and higher sustained levels of disturbance.

4.4 | Future research priorities

Repeat LiDAR data has the both the scale and sensitivity needed to measure disturbance and recovery in tropical forests. However, collecting airborne LiDAR data are expensive as it requires the use of an aircraft and costly sensors. We therefore believe that future research opportunities lie in combining more frequent LiDAR data collection with regular low-cost drone monitoring and high-resolution satellite imagery. This increased temporal resolution would help us better understand the drivers of disturbance and recovery (Araujo et al., 2021; Simonetti et al., 2023). In addition, this would help us track small gaps, many of which are likely to have both formed and recovered within the 4–5-year interval between LiDAR scans, and better account for potential confounding factors such as leaf phenology.

The cost of repeat LiDAR data also limits its spatial coverage. In this study, we could not find any repeat LiDAR data for the Western Amazon, where productivity and mortality rates are higher than the regions we studied (Malhi et al., 2004), or for West and Central African forests, which are a crucial part of the terrestrial carbon cycle (Bennett et al., 2021). Field-based gap dynamics studies showed that African forests had slower turnover rates than those in central and South America (Jans et al., 1993), but it would be extremely valuable to test this over larger scales using modern methods. This problem could potentially be overcome by coupling space-borne LiDAR (Duncanson et al., 2022; Holcomb et al., 2023, 2024) to track forest recovery with regular high-resolution (<5 m) satellite optical imagery to track forest disturbance (Dalagnol et al., 2023). However, we believe that periodic airborne LiDAR data, processed using robust pipelines (Fischer et al., 2024), will be invaluable in measuring landscape-scale forest dynamics for the foreseeable future.

AUTHOR CONTRIBUTIONS

Toby D. Jackson: Conceptualization; data curation; formal analysis; funding acquisition; methodology; project administration;

validation; visualization; writing – original draft; writing – review and editing. **Fabian J. Fischer:** Data curation; methodology; validation; writing – review and editing. **Grégoire Vincent:** Data curation; funding acquisition; methodology; writing – review and editing. **Eric B. Gorgens:** Data curation; methodology; writing – review and editing. **Michael Keller:** Data curation; writing – review and editing. **Jérôme Chave:** Writing – review and editing. **Tommaso Jucker:** Data curation; methodology; writing – review and editing. **David A. Coomes:** Conceptualization; methodology; project administration; writing – review and editing.

ACKNOWLEDGMENTS

TJa and DC were supported by project NE/S010750/1, which also funded the 2019 LiDAR data collection in French Guiana (collected by Altoa) and the 2020 data collection in Malaysia (collected by Ground Data Solutions). We thank the Danum Valley Management Committee and Sabah Biodiversity Council for access and assistance with the LiDAR surveys in Malaysia. TJu was supported by a UK NERC Independent Research Fellowship (grant: NE/S01537X/1), through a Research Project Grant from the Leverhulme Trust which also funded FJF (grant code: RPG-2020-341), and a UK NERC Standard Grant, which also supported TJa (NE/X000281/1). We also thank the Sustainable Landscapes Brazil project supported by the Brazilian Agricultural Research Corporation (EMBRAPA), the US Forest Service, USAID and the US Department of State, for providing the multi-temporal airborne lidar dataset. This study benefited from an 'Investissement d'Avenir' grant managed by the Agence Nationale de la Recherche (CEBA, ref. ANR-10-LABX-25-01; TULIP, ref. ANR-10-LABX-0041; ANAEE-France: ANR-11-INBS-0001), CNES Biomass-Valo project and ESA CCI-BIOMASS. For the purpose of open access, the author(s) has applied a Creative Commons Attribution (CC BY) licence to any Author Accepted Manuscript version arising from this submission.

CONFLICT OF INTEREST STATEMENT

The authors declare no conflicts of interests for this article.

DATA AVAILABILITY STATEMENT

The data that support the findings of this study are openly available on Zenodo at https://doi.org/10.5281/zenodo.10908679. The R code to process these canopy height models and produce the figures is available on Github: https://github.com/TobyDJackson/Forest_disturbance_and_recovery_LiDAR and released on Zenodo https://doi.org/10.5281/zenodo.13234994.

The underlying LiDAR point cloud data is openly available:

- Danum 2014: https://data.ceda.ac.uk/neodc/arsf/2014/MA14_11.
- Sepilok 2014: https://data.ceda.ac.uk/neodc/arsf/2014/MA14_14.
- Danum and Sepilok 2020: https://doi.org/10.5285/dd4d20c8626f4b9d99bc14358b1b50fe.
- Nouragues 2019: https://doi.org/10.5285/7bdc5bfc06264802be34f918597150e8.
- Paracou 2019: https://doi.org/10.5285/1d554ff41c104491ac3661c6f6f52aab.
- Tapajós and Ducke are available here https://www.paisagenslidar.cnptia.embrapa.br/ and also here https://doi.org/10.3334/ORNLDAAC/1644.

ORCID

Toby D. Jackson https://orcid.org/0000-0001-8143-6161
Fabian J. Fischer https://orcid.org/0000-0003-2325-9886
Grégoire Vincent https://orcid.org/0000-0001-9443-021X
Eric B. Gorgens https://orcid.org/0000-0003-2517-0279
Michael Keller https://orcid.org/0000-0002-0253-3359
Jérôme Chave https://orcid.org/0000-0002-7766-1347
Tommaso Jucker https://orcid.org/0000-0002-0751-6312
David A. Coomes https://orcid.org/0000-0002-8261-2582

REFERENCES

Araujo, R. F., Grubinger, S., Celes, C. H. S., Negrón-Juárez, R., Garcia, M., Dandois, J., & Muller-Landau, H. (2021). Strong temporal variation in treefall and branchfall rates in a tropical forest is explained by rainfall: Results from five years of monthly drone data for a 50-ha plot. *Biogeosciences Discussions*, *20*, 1–19. https://doi.org/10.5194/BG-2021-102

Ashton, P. (2014). *On the forests of tropical Asia lest the memory fade*. Kew Publishing.

Banin, L., Lewis, S. L., Lopez-Gonzalez, G., Baker, T. R., Quesada, C. A., Chao, K.-J., Burslem, D. F. R. P., Nilus, R., Abu Salim, K., Keeling, H. C., Tan, S., Davies, S. J., Monteagudo Mendoza, A., Vásquez, R., Lloyd, J., Neill, D. A., Pitman, N., & Phillips, O. L. (2014). Tropical forest wood production: A cross-continental comparison. *Journal of Ecology*, *102*(4), 1025–1037. https://doi.org/10.1111/1365-2745.12263

Bennett, A. C., Dargie, G. C., Cuni-Sanchez, A., Mukendi, J. T., Hubau, W., Mukinzi, J. M., Phillips, O. L., Malhi, Y., Sullivan, M. J. P., Cooper, D. L. M., Adu-Bredu, S., Affum-Baffoe, K., Amani, C. A., Banin, L. F., Beeckman, H., Begne, S. K., Bocko, Y. E., Boeckx, P., Bogaert, J., … Lewis, S. L. (2021). Resistance of African tropical forests to an extreme climate anomaly. *Proceedings of the National Academy of Sciences*, *118*(21), e2003169118. https://doi.org/10.1073/pnas.2003169118

Bennett, A. C., Rodrigues de Sousa, T., Monteagudo-Mendoza, A., Esquivel-Muelbert, A., Morandi, P. S., Coelho de Souza, F., Castro, W., Duque, L. F., Llampazo, G. F., & Manoel dos Santos, R. (2023). Sensitivity of South American tropical forests to an extreme climate anomaly. *Nature Climate Change*, *13*(9), 967–974.

Berenguer, E., Lennox, G. D., Ferreira, J., Malhi, Y., Aragão, L. E. O. C., Barreto, J. R., Del Bon Espírito-Santo, F., Figueiredo, A. E. S., França, F., Gardner, T. A., Joly, C. A., Palmeira, A. F., Quesada, C. A., Rossi, L. C., de Seixas, M. M. M., Smith, C. C., Withey, K., & Barlow, J. (2021). Tracking the impacts of El Niño drought and fire in human-modified Amazonian forests. *Proceedings of the National Academy of Sciences*, *118*(30), e2019377118. https://doi.org/10.1073/pnas.2019377118

Brokaw, N. V. L. (1982). The definition of treefall gap and its effect on measures of forest dynamics. *Biotropica*, *14*, 158–160.

Bugmann, H., Seidl, R., Hartig, F., Bohn, F., Brůna, J., Cailleret, M., François, L., Heinke, J., Henrot, A.-J., Hickler, T., Hülsmann, L., Huth, A., Jacquemin, I., Kollas, C., Lasch-Born, P., Lexer, M. J., Merganič, J., Merganičová, K., Mette, T., … Reyer, C. P. O. (2019). Tree mortality submodels drive simulated long-term forest dynamics: Assessing 15 models from the stand to global scale. *Ecosphere*, *10*(2), e02616. https://doi.org/10.1002/ecs2.2616

Cabon, A., Kannenberg, S. A., Arain, A., Babst, F., Baldocchi, D., Belmecheri, S., Delpierre, N., Guerrieri, R., Maxwell, J. T., McKenzie, S., Meinzer, F. C., Moore, D. J. P., Pappas, C., Rocha, A. V., Szejner, P., Ueyama, M., Ulrich, D., Vincke, C., Voelker, S. L., … Anderegg, W. R. L. (2022). Cross-biome synthesis of source versus sink limits to tree growth. *Science*, *376*(6594), 758–761. https://doi.org/10.1126/science.abm4875

Chave, J., Coomes, D., Jansen, S., Lewis, S. L., Swenson, N. G., & Zanne, A. E. (2009). Towards a worldwide wood economics spectrum. *Ecology Letters*, *12*(4), 351–366. https://doi.org/10.1111/j.1461-0248.2009.01285.x

Chave, J., Piponiot, C., Maréchaux, I., de Foresta, H., Larpin, D., Fischer, F. J., Derroire, G., Vincent, G., & Hérault, B. (2020). Slow rate of secondary forest carbon accumulation in the Guianas compared with the rest of the Neotropics. *Ecological Applications*, *30*(1), e02004. https://doi.org/10.1002/eap.2004

Clark, D. B., Clark, D. A., & Kellner, J. R. (2022). Spatial and temporal scales of canopy disturbance and recovery across an old-growth tropical rain forest landscape. *Ecological Monographs*, *92*(1), e01496. https://doi.org/10.1002/ecm.1496

Coomes, D., & Jackson, T. (2022). *Airborne LiDAR and RGB imagery from Sepilok reserve and Danum Valley in Malaysia in 2020* [Dataset]. NERC EDS Centre for Environmental Data Analysis. https://doi.org/10.5285/DD4D20C8626F4B9D99BC14358B1B50FE

Cushman, K. C., Detto, M., García, M., & Muller-Landau, H. C. (2022). Soils and topography control natural disturbance rates and thereby forest structure in a lowland tropical landscape. *Ecology Letters*, *25*(5), 1126–1138.

Dalagnol, R., Wagner, F. H., Galvão, L. S., Braga, D., Osborn, F., Sagang, L. B., da Conceição Bispo, P., Payne, M., Junior, C. S., Favrichon, S., Silgueiro, V., Anderson, L. O., Oliveira e Cruz de Aragão, L. E., Fensholt, R., Brandt, M., & Ciais, P. (2023). Mapping tropical forest degradation with deep learning and planet NICFI data. *Remote Sensing of Environment*, *298*(December), 113798. https://doi.org/10.1016/j.rse.2023.113798

de Lima, R. A. F., Phillips, O. L., Duque, A., Tello, J. S., Davies, S. J., de Oliveira, A. A., Muller, S., Honorio Coronado, E. N., Vilanova, E., & Cuni-Sanchez, A. (2022). Making forest data fair and open. *Nature Ecology & Evolution*, *6*(6), 656–658.

de Reu, J., Bourgeois, J., Bats, M., Zwertvaegher, A., Gelorini, V., de Smedt, P., Chu, W., Antrop, M., de Maeyer, P., Finke, P., van Meirvenne, M., Verniers, J., & Crombé, P. (2013). Application of the topographic position index to heterogeneous landscapes. *Geomorphology*, *186*(March), 39–49. https://doi.org/10.1016/j.geomorph.2012.12.015

Denslow, J. S. (1987). Tropical rainforest gaps and tree species diversity. *Annual Review of Ecology and Systematics*, *18*, 431–451.

dos-Santos, M. N., Keller, M. M., & Morton, D. C. (2019). *LiDAR surveys over selected Forest research sites, Brazilian Amazon, 2008–2018* [Dataset]. ORNL DAAC. https://doi.org/10.3334/ORNLDAAC/1644

Duncanson, L., Kellner, J. R., Armston, J., Dubayah, R., Minor, D. M., Hancock, S., Healey, S. P., Patterson, P. L., Saarela, S., Marselis, S., Silva, C. E., Bruening, J., Goetz, S. J., Tang, H., Hofton, M., Blair, B., Luthcke, S., Fatoyinbo, L., Abernethy, K., … Zgraggen, C. (2022). Aboveground biomass density models for NASA's Global Ecosystem Dynamics Investigation (GEDI) lidar mission. *Remote Sensing of Environment*, *270*(March), 112845. https://doi.org/10.1016/j.rse.2021.112845

Espírito-Santo, F. D. B., Gloor, M., Keller, M., Malhi, Y., Saatchi, S., Nelson, B., Oliveira Junior, R. C., Pereira, C., Lloyd, J., Frolking, S., Palace, M., Shimabukuro, Y. E., Duarte, V., Mendoza, A. M., López-González, G., Baker, T. R., Feldpausch, T. R., Brienen, R. J., Asner, G. P., … Phillips, O. L. (2014). Size and frequency of natural forest disturbances and the Amazon forest carbon balance. *Nature Communications*, *5*(March), 3434. https://doi.org/10.1038/ncomms4434

Fischer, F. J., Jackson, T. D., Vincent, G., & Jucker, T. (2024). Robust characterization of forest structure from airborne laser scanning—A systematic assessment and sample workflow for ecologists. *bioRxiv*. https://doi.org/10.1101/2024.03.27.586702

Gloor, M., Phillips, O. L., Lloyd, J. J., Lewis, S. L., Malhi, Y., Baker, T. R., López-Gonzalez, G., Peacock, J., Almeida, S., de Oliveira, A. A., Alvarez, E., Amaral, I., Arroyo, L., Aymard, G., Banki, O., Blanc, L., Bonal, D., Brando, P., Chao, K.-J., … van der Heijden, G. (2009). Does the disturbance hypothesis explain the biomass increase in basin-wide Amazon forest plot data? *Global Change Biology*, *15*(10), 2418–2430. https://doi.org/10.1111/j.1365-2486.2009.01891.x

Goodwin, N. R., Coops, N. C., & Culvenor, D. S. (2006). Assessment of forest structure with airborne LiDAR and the effects of platform altitude. *Remote Sensing of Environment*, *103*(2), 140–152. https://doi.org/10.1016/j.rse.2006.03.003

Gora, E. M., & Esquivel-Muelbert, A. (2021). Implications of size-dependent tree mortality for tropical forest carbon dynamics. *Nature Plants*, *7*(4), 384–391. https://doi.org/10.1038/s41477-021-00879-0

Gorgens, E. B., Keller, M., Jackson, T., Marra, D. M., Reis, C. R., de Almeida, D. R. A., Coomes, D., & Ometto, J. P. (2023). Out of steady state: Tracking canopy gap dynamics across Brazilian Amazon. *Biotropica*, *55*(4), 755–766. https://doi.org/10.1111/btp.13226

Gorgens, E. B., Keller, M., Jackwon, T. D., Marra, D. M., Reis, C. R., Almeida, D. R. A., Coomes, D., & Ometto, J. P. (2022). Tracking canopy gap dynamics across four sites in the Brazilian Amazon. *bioRxiv*. https://doi.org/10.1101/2022.09.03.506473

Hijmans, R. J., Bivand, R., Forner, K., Ooms, J., Pebesma, E., & Sumner, M. D. (2022). *Package 'Terra'*. Maintainer.

Holcomb, A., Burns, P., Keshav, S., & Coomes, D. A. (2024). Repeat GEDI footprints measure the effects of tropical forest disturbances. *Remote Sensing of Environment*, *308*(July), 114174. https://doi.org/10.1016/j.rse.2024.114174

Holcomb, A., Mathis, S. V., Coomes, D. A., & Keshav, S. (2023). Computational tools for assessing forest recovery with GEDI shots and forest change maps. *Science of Remote Sensing*, *8*(December), 100106. https://doi.org/10.1016/j.srs.2023.100106

Hubau, W., Lewis, S. L., Phillips, O. L., Affum-Baffoe, K., Beeckman, H., Cuní-Sanchez, A., Daniels, A. K., Ewango, C. E. N., Fauset, S., Mukinzi, J. M., Sheil, D., Sonké, B., Sullivan, M. J. P., Sunderland, T. C. H., Taedoumg, H., Thomas, S. C., White, L. J. T., Abernethy, K. A., Adu-Bredu, S., … Zemagho, L. (2020). Asynchronous carbon sink saturation in African and Amazonian tropical forests. *Nature*, *579*(7797), 80–87. https://doi.org/10.1038/s41586-020-2035-0

Hunter, M. O., Keller, M., Morton, D., Cook, B., Lefsky, M., Ducey, M., Saleska, S., Cosme de Oliveira, R., Jr., & Schietti, J. (2015). Structural dynamics of tropical moist forest gaps. *PLoS One*, *10*(7), e0132144.

IPCC. (2021). *IPCC, 2022: Climate change 2022: Impacts, adaptation, and vulnerability. Contribution of working group II to the sixth assessment report of the intergovernmental panel on climate change*. Cambridge University Press.

Jackson, T. (2024). *TobyDJackson/Forest_disturbance_and_recovery_LiDAR: 1.0 (v1.0)* [Computer software]. Zenodo. https://doi.org/10.5281/zenodo.13234995

Jackson, T., Fischer, F., Vincent, G., Gorgens, E., Keller, M., Chave, J., Jucker, T., & Coomes, D. (2024). *Repeat LiDAR canopy height models for Borneo, eastern Amazon and Guiana Shield* [Dataset]. Zenodo. https://doi.org/10.5281/zenodo.10908679

Jackson, T., Shenkin, A. F., Majalap, N., Bin Jami, J., Bin Sailim, A., Reynolds, G., Coomes, D. A., Chandler, C. J., Boyd, D. S., Burt, A., Wilkes, P., Disney, M., & Malhi, Y. (2020). The mechanical stability of the world's tallest broadleaf trees. *Biotropica*, *53*(1), 110–120. https://doi.org/10.1111/btp.12850

Jackson, T., Vincent, G., & Coomes, D. (2023a). *Aerial LiDAR data from French Guiana, Nouragues, November 2019* (p. 496 Files, 17314432487 B) [Dataset]. NERC EDS Centre for Environmental Data Analysis. https://doi.org/10.5285/7BDC5BFC06264802BE34F918597150E8

Jackson, T., Vincent, G., & Coomes, D. (2023b). *Aerial LiDAR data from French Guiana, Paracou, November 2019* (p. 183 Files, 7507934852

B) [Dataset]. NERC EDS Centre for Environmental Data Analysis. https://doi.org/10.5285/1D554FF41C104491AC3661C6F6F52AAB

Jans, L., Poorter, L., Renaat, S. A. R. v. R., & Bongers, F. (1993). Gaps and forest zones in tropical moist forest in Ivory Coast. *Biotropica*, *25*, 258–269.

Jansen, P. A., van der Meer, P. J., & Bongers, F. (2008). Spatial contagiousness of canopy disturbance in tropical rain forest: An individual-tree-based test. *Ecology*, *89*(12), 3490–3502. https://doi.org/10.1890/07-1682.1

Jucker, T. (2022). Deciphering the fingerprint of disturbance on the three-dimensional structure of the world's forests. *New Phytologist*, *233*(2), 612–617. https://doi.org/10.1111/nph.17729

Jucker, T., Asner, G. P., Dalponte, M., Brodrick, P. G., Philipson, C. D., Vaughn, N. R., Teh, Y. A., Brelsford, C., Burslem, D. F. R. P., Deere, N. J., Ewers, R. M., Kvasnica, J., Lewis, S. L., Malhi, Y., Milne, S., Nilus, R., Pfeifer, M., Phillips, O. L., Qie, L., … Coomes, D. A. (2018). Estimating aboveground carbon density and its uncertainty in Borneo's structurally complex tropical forests using airborne laser scanning. *Biogeosciences*, *15*(12), 3811–3830. https://doi.org/10.5194/bg-15-3811-2018

Jucker, T., Bongalov, B., Burslem, D. F. R. P., Nilus, R., Dalponte, M., Lewis, S. L., Phillips, O. L., Qie, L., & Coomes, D. A. (2018). Topography shapes the structure, composition and function of tropical forest landscapes. *Ecology Letters*, *21*, 989–1000. https://doi.org/10.1111/ele.12964

Kannenberg, S. A., Cabon, A., Babst, F., Belmecheri, S., Delpierre, N., Guerrieri, R., Maxwell, J. T., Meinzer, F. C., Moore, D. J. P., Pappas, C., Ueyama, M., Ulrich, D. E. M., Voelker, S. L., Woodruff, D. R., & Anderegg, W. R. L. (2022). Drought-induced decoupling between carbon uptake and tree growth impacts forest carbon turnover time. *Agricultural and Forest Meteorology*, *322*(July), 108996. https://doi.org/10.1016/j.agrformet.2022.108996

Körner, C. (2003). Slow in, rapid out—Carbon flux studies and Kyoto targets. *Science*, *300*(5623), 1242–1243. https://doi.org/10.1126/science.1084460

Krüger, K., Senf, C., Jucker, T., Pflugmacher, D., & Seidl, R. (2024). Gap expansion is the dominant driver of canopy openings in a temperate mountain forest landscape. *Journal of Ecology*, *112*, 1501–1515. https://doi.org/10.1111/1365-2745.14320

Leitold, V., Morton, D. C., Longo, M., Dos-Santos, M. N., Keller, M., & Scaranello, M. (2018). El Niño drought increased canopy turnover in Amazon forests. *New Phytologist*, *219*, 959–971. https://doi.org/10.1111/nph.15110

Leitold, V., Morton, D. C., Martinuzzi, S., Paynter, I., Uriarte, M., Keller, M., Ferraz, A., Cook, B. D., Corp, L. A., & González, G. (2022). Tracking the rates and mechanisms of canopy damage and recovery following Hurricane Maria using multitemporal lidar data. *Ecosystems*, *25*(4), 892–910. https://doi.org/10.1007/s10021-021-00688-8

Malhi, Y., Baker, T. R., Phillips, O. L., Almeida, S., Alvarez, E., Arroyo, L., Chave, J., Czimczik, C. I., Fiore, A. D., Higuchi, N., Killeen, T. J., Laurance, S. G., Laurance, W. F., Lewis, S. L., Montoya, L. M. M., Monteagudo, A., Neill, D. A., Vargas, P. N., Patiño, S., … Lloyd, J. (2004). The above-ground coarse wood productivity of 104 neotropical forest plots. *Global Change Biology*, *10*(5), 563–591. https://doi.org/10.1111/j.1529-8817.2003.00778.x

Marvin, D. C., & Asner, G. P. (2016). Branchfall dominates annual carbon flux across lowland Amazonian forests. *Environmental Research Letters*, *11*(9), 094027.

Mitchard, E. T. A. (2018). The tropical forest carbon cycle and climate change. *Nature*, *559*(7715), 527–534. https://doi.org/10.1038/s41586-018-0300-2

Mitchard, E. T. A., Feldpausch, T. R., Brienen, R. J. W., Lopez-Gonzalez, G., Monteagudo, A., Baker, T. R., Lewis, S. L., Lloyd, J., Quesada, C. A., Gloor, M., ter Steege, H., Meir, P., Alvarez, E., Araujo-Murakami, A., Aragão, L. E. O. C., Arroyo, L., Aymard, G., Banki, O., Bonal, D., … Phillips, O. L. (2014). Markedly divergent estimates of Amazon forest carbon density from ground plots and satellites. *Global Ecology and Biogeography*, *23*(8), 935–946. https://doi.org/10.1111/geb.12168

Morsdorf, F., Frey, O., Meier, E., Itten, K. I., & Allgöwer, B. (2008). Assessment of the influence of flying altitude and scan angle on biophysical vegetation products derived from airborne laser scanning. *International Journal of Remote Sensing*, *29*(5), 1387–1406. https://doi.org/10.1080/01431160701736349

Muller-Landau, H. C., Cushman, K. C., Arroyo, E. E., Cano, I. M., Anderson-Teixeira, K. J., & Backiel, B. (2021). Patterns and mechanisms of spatial variation in tropical forest productivity, woody residence time, and biomass. *New Phytologist*, *229*(6), 3065–3087. https://doi.org/10.1111/nph.17084

Næsset, E. (2009). Effects of different sensors, flying altitudes, and pulse repetition frequencies on forest canopy metrics and biophysical stand properties derived from small-footprint airborne laser data. *Remote Sensing of Environment*, *113*(1), 148–159. https://doi.org/10.1016/j.rse.2008.09.001

Negrón-Juárez, R. I., Chambers, J. Q., Guimaraes, G., Zeng, H., Raupp, C. F. M., Marra, D. M., Ribeiro, G. H. P. M., Saatchi, S. S., Nelson, B. W., & Higuchi, N. (2010). Widespread Amazon forest tree mortality from a single cross-basin squall line event. *Geophysical Research Letters*, *37*(16), 34–39. https://doi.org/10.1029/2010GL043733

Nunes, M. H., Jucker, T., Riutta, T., Svátek, M., Kvasnica, J., Rejžek, M., Matula, R., Majalap, N., Ewers, R. M., Swinfield, T., Valbuena, R., Vaughn, N. R., Asner, G. P., & Coomes, D. A. (2021). Recovery of logged forest fragments in a human-modified tropical landscape during the 2015–16 El Niño. *Nature Communications*, *12*(1), 1526. https://doi.org/10.1038/s41467-020-20811-y

Phillips, O. L., Lewis, S. L., Baker, T. R., Chao, K.-J., & Higuchi, N. (2008). The changing Amazon forest. *Philosophical Transactions of the Royal Society, B: Biological Sciences*, *363*(1498), 1819–1827. https://doi.org/10.1098/rstb.2007.0033

Piponiot, C., Anderson-Teixeira, K. J., Davies, S. J., Allen, D., Bourg, N. A., Burslem, D. F. R. P., Cárdenas, D., Chang-Yang, C.-H., Chuyong, G., Cordell, S., Dattaraja, H. S., Duque, Á., Ediriweera, S., Ewango, C., Ezedin, Z., Filip, J., Giardina, C. P., Howe, R., Hsieh, C.-F., … Muller-Landau, H. C. (2022). Distribution of biomass dynamics in relation to tree size in forests across the world. *New Phytologist*, *234*(5), 1664–1677. https://doi.org/10.1111/nph.17995

Qie, L., Lewis, S. L., Sullivan, M. J. P., Lopez-Gonzalez, G., Pickavance, G. C., Sunderland, T., Ashton, P., Hubau, W., Abu Salim, K., Aiba, S.-I., Banin, L. F., Berry, N., Brearley, F. Q., Burslem, D. F. R. P., Dančák, M., Davies, S. J., Fredriksson, G., Hamer, K. C., Hédl, R., … Phillips, O. L. (2017). Long-term carbon sink in Borneo's forests halted by drought and vulnerable to edge effects. *Nature Communications*, *8*(1), 1966. https://doi.org/10.1038/s41467-017-01997-0

Quesada, C. A., Lloyd, J., Schwarz, M., Patiño, S., Baker, T. R., Czimczik, C., Fyllas, N. M., Martinelli, L., Nardoto, G. B., Schmerler, J., Santos, A. J. B., Hodnett, M. G., Herrera, R., Luizão, F. J., Arneth, A., Lloyd, G., Dezzeo, N., Hilke, I., Kuhlmann, I., … Paiva, R. (2010). Variations in chemical and physical properties of Amazon forest soils in relation to their genesis. *Biogeosciences*, *7*(5), 1515–1541. https://doi.org/10.5194/bg-7-1515-2010

R Core Team. (2021). *R: A language and environment for statistical computing*. R Foundation for Statistical Computing. https://www.R-project.org/

Reiche, J., Mullissa, A., Slagter, B., Gou, Y., Tsendbazar, N.-E., Odongo-Braun, C., Vollrath, A., Weisse, M. J., Stolle, F., Pickens, A., Donchyts, G., Clinton, N., Gorelick, N., & Herold, M. (2021). Forest disturbance alerts for the Congo Basin using Sentinel-1. *Environmental Research Letters*, *16*(2), 024005. https://doi.org/10.1088/1748-9326/abd0a8

Rifai, S. W., Girardin, C. A. J., Berenguer, E., del Aguila-Pasquel, J., Dahlsjö, C. A. L., Doughty, C. E., Jeffery, K. J., Moore, S., Oliveras, I., Riutta, T., Rowland, L. M., Murakami, A. A., Addo-Danso, S. D., Brando, P., Burton, C., Ondo, F. E., Duah-Gyamfi, A., Amézquita, F. F., Freitag, R., … Malhi, Y. (2018). ENSO drives interannual variation of forest woody growth across the tropics. *Philosophical Transactions of the Royal Society*, *B: Biological Sciences*, *373*(1760), 20170410. https://doi.org/10.1098/rstb.2017.0410

Rifai, S. W., Li, S., & Malhi, Y. (2019). Coupling of El Niño events and long-term warming leads to pervasive climate extremes in the terrestrial tropics. *Environmental Research Letters*, *14*(10), 105002. https://doi.org/10.1088/1748-9326/ab402f

Roussel, J.-R., Caspersen, J., Béland, M., Thomas, S., & Achim, A. (2017). Removing bias from LiDAR-based estimates of canopy height: Accounting for the effects of pulse density and footprint size. *Remote Sensing of Environment*, *198*(September), 1–16. https://doi.org/10.1016/J.RSE.2017.05.032

Shenkin, A., Chandler, C., Boyd, D., Jackson, T., Disney, M., Majalap, N., Nilus, R., Foody, G., Bin Jami, J., Reynolds, G., Wilkes, P., Cutler, M. E. J., van der Heijden, G. M. F., Burslem, D. F. R. P., Coomes, D. A., Bentley, L. P., & Malhi, Y. (2019). The world's tallest tropical tree in three dimensions. *Frontiers in Forests and Global Change*, *2*, 32. https://doi.org/10.3389/FFGC.2019.00032

Silva, C. A., Valbuena, R., Pinagé, E. R., Mohan, M., de Almeida, D. R. A., Broadbent, E. N., Jaafar, W. S. W. M., de Almeida Papa, D., Cardil, A., & Klauberg, C. (2019). ForestGapR: An r package for forest gap analysis from canopy height models. *Methods in Ecology and Evolution*, *10*(8), 1347–1356. https://doi.org/10.1111/2041-210X.13211

Simonetti, A., Araujo, R. F., Celes, C. H. S., da Silva e Silva, F. R., dos Santos, J., Higuchi, N., Trumbore, S., & Marra, D. M. (2023). Canopy gaps and associated losses of biomass—Combining UAV imagery and field data in a central Amazon forest. *Biogeosciences*, *20*(17), 3651–3666. https://doi.org/10.5194/bg-20-3651-2023

Steege, T., Hans, N. C. A., Pitman, O. L., Phillips, J. C., Sabatier, D., Duque, A., Molino, J.-F., Prévost, M.-F., Spichiger, R., & Castellanos, H. (2006). Continental-scale patterns of canopy tree composition and function across Amazonia. *Nature*, *443*(7110), 444–447.

Vancutsem, C., Achard, F., Pekel, J.-F., Vieilledent, G., Carboni, S., Simonetti, D., Gallego, J., Aragão, L. E. O. C., & Nasi, R. (2021). Long-term (1990–2019) monitoring of forest cover changes in the humid tropics. *Science Advances*, *7*(10), eabe1603. https://doi.org/10.1126/sciadv.abe1603

Wagner, F., Rossi, V., Stahl, C., Bonal, D., & Herault, B. (2012). Water availability is the main climate driver of neotropical tree growth. *PLoS One*, *7*(4), e34074.

SUPPORTING INFORMATION

Additional supporting information can be found online in the Supporting Information section at the end of this article.

How to cite this article: Jackson, T. D., Fischer, F. J., Vincent, G., Gorgens, E. B., Keller, M., Chave, J., Jucker, T., & Coomes, D. A. (2024). Tall Bornean forests experience higher canopy disturbance rates than those in the eastern Amazon or Guiana shield. *Global Change Biology*, *30*, e17493. https://doi.org/10.1111/gcb.17493